THE AERODYNAMIC PERFORMANCE OF A THRUST REVERSER CASCADE

H. Yao, J. Butterfield, S. Raghunathan, R. Cooper and E. Benard
School of Aeronautical Engineering,
Queen's University Belfast, UK

Keywords: *thrust reverser, cascade, unsteady compressible flow, aerodynamics*

Abstract

A key component of an aircraft power plant system is the thrust reverser. The thrust reverser considered in this paper uses the natural blockage concept, with only the fan duct flow being reversed. This paper focuses on the study of the aerodynamic performance of the cascade within a cold stream thrust reverser. Aerodynamic simulations are carried out using realistic operating conditions, for idealized cascade models representing three design options. The aim of this work is to investigate whether the aerodynamic performance of the thrust reverser cascade has been improved while minimizing weight of the cascade.

The numerical simulations show that despite a reduction in total reverse thrust for the weight reduced designs, the supersonic flow regime, which existed in the original design, was eliminated after changing vane configurations made with the 5% and 10% weight reductions. The aerodynamic performance around the cascade and in the fan duct within the thrust reverser has been improved. The total reverse thrust is not significantly affected with the modified cascade.

1 Introduction

In modern aircraft the thrust reverser is built in to the engine nacelle. A thrust reverser uses the power of a jet engine as a deceleration force by reversing the direction of airflow, which generates forward thrust. Fig. 1 shows a section through jet engine with a typical cold stream thrust reverser. Some of the thrust reversers employ a cascade to enhance the turning of the flow [1]. Thrust reversers significantly affect nacelle design increasing weight and resulting in higher manufacturing and operational costs. A key component of an aircraft power-plant system is the thrust reverser. Any reduction in the weight of aircraft components will reduce fuel consumption resulting in lower operational costs [2].

A thrust reverser offers a number of operational advantages. Some of the advantages of having a thrust reverser are as follows [3]:

- Shortening of landing runs
- less wear and tear of aircraft brakes
- safer landing in adverse weather conditions
- additional safety and control margins during aborted take-offs

There are broadly two types of thrust reversers [4]:

(a) using both core flow and fan flow;
(b) using fan flow only.

The thrust reverser considered in this paper uses the natural blockage concept and reverse fan flow only. The schematic sketch of the thrust reverser is presented in Fig. 2 for the deployed configuration.

The high pressure and velocity within the nacelle system during reverse thrust can lead to supersonic and turbulent flow regimes within the structure. These factors can lead to issues with the strength and durability of nacelle components such as the cascade. The

aim of this work is to minimize weight while maintaining or improving aerodynamic performance. To illustrate how component design can be improved, it is important to investigate whether the aerodynamic performance on components of the nacelle system has been improved.

In this paper, a cascade has been assessed using computational fluid dynamics (CFD) methods. Three designs of a thrust reverser cascade are put into practice with a view to reducing weight [5] (see Fig. 3). The Aerodynamic performances around the cascade and in the fan duct within the thrust reverser have been studied. The numerical results show that the flow fields in the fan duct and around the cascade have been improved, although total reverse thrust is reduced by 2.5% and 2.2% for both of the reduced weight designs. The total reverse thrust is not significantly affected with the modified cascade.

2 Methodology

Time-dependent viscous compressible flows through a thrust reverser computational model (see Figure.2) have been simulated using the commercial CFD flow solver, FLUENT. The governing integral equations are solved by FLUENT with the finite volume approach. The system of equations is cast integral, Cartesian form for an arbitrary control volume V with differential surface area A as follows:

$$\frac{\partial}{\partial t}\int_V W dV + \oint [F - G]\cdot dA = 0 \qquad (1)$$

where the vectors W, F, and G are defined as

$$W = \begin{Bmatrix} \rho \\ \rho u \\ \rho v \\ \rho E \end{Bmatrix} \quad F = \begin{Bmatrix} \rho\vec{u} \\ \rho\vec{u}u + p\vec{i} \\ \rho\vec{u}v + p\vec{j} \\ \rho\vec{u}E + p\vec{u} \end{Bmatrix} \quad G = \begin{Bmatrix} 0 \\ \tau_{xi} \\ \tau_{yi} \\ \tau_{ij}u_j + q \end{Bmatrix}$$

Here ρ, $\vec{u} = (u, v)$, E, and p are the density, velocity, total energy per unit mass, and pressure of the fluid, respectively. τ is the viscous stress tensor, and q is the heat flux. Total energy E is related to the total enthalpy H by

$$E = H - p/\rho \qquad (2)$$

and

$$H = h + |\vec{u}|^2/2 \qquad (3)$$

The Reynolds-Averaged approach with the RNG (renormalization group) k-ε model has been used to model the effect of turbulence. The RNG k-ε model is derived from the instantaneous Navier-Stokes equations, using a mathematical technique called "renormalization group" methods. The analytical derivation results in a model with constants different from those in the standard k-ε model, and additional terms and functions in the transport equations for k and ε.

3 Validation

The CFD predictions presented in this paper for the baseline model (see Fig. 2) was validated against wind tunnel test data collected at Flow Science Ltd, Manchester, UK, by Bombardier Aerospace Shorts during 1998 on a 40% scale model of the nature block thrust reverser [6].

To validate the computational solution further, the unstructured non-uniform grid was increased from *30,000* cells to *90,000* cells for the baseline model. Specifically, 2-D grids are generated with clustering of nodes near wall regions (see Fig. 4). The pressure-far-field, the pressure-inlet and the pressure-outlet boundary conditions were defined for an ISA Sea Level atmosphere (i.e. 15° C) and Mach number (M) of 0.2.

It is found that there is no significant difference between the solutions of those two

grid systems showing that they are grid independent [6].

4 Results and Discussion

The aerodynamic performances of three designs for the cascade of the thrust reverser have been investigated. Design 1 is the original cascade [6] (see Fig. 3 (a)). Two modifications (i.e. Design 2 and Design 3) were made to the vane configuration to determine if cascade weight could be reduced. Both of these changes involved making the vanes in predicted high pressure areas, larger and heavier and making the vanes in predicted low pressure areas smaller and lighter. The net effect was a reduction of 5% in weight for Design 2 (see Fig. 3 (b)), and a reduction of 10% for Design 3 (see Fig. 3 (c)) [5]. The computational conditions used for predicting aerodynamic performances of those three designs are the same as described in Section 3.

Fig. 5(a) shows the static pressure distribution in the fan duct and around the cascade for Design 1. The higher pressures occur to the right of the cascade section where the flow is physically blocked and re-directed through the cascade. Fig. 5(b) and (c) show the static pressure distributions obtained for Design 2 and Design 3 for the same operational conditions. The increase in area through the cascade, brought about by changing the vane configuration and introducing 'slots' through Vane 11, results in lower exit pressure peak around Vanes 10 and 11. As evidence Fig. 6 presents the pressure distributions around Vane 11 for three designs. Fig. 6 shows that the pressure peak around Vane 11 for both Design 2 and 3 has been reduced. It means that the pressure distributions around it have been improved. The static pressure distributions shown in Fig. 5 have transferred and used in the structural analysis by finite element approach (FEA) [5].

The total reverse thrust produced by the thrust reverser for those three cascade configurations have been compared in Fig. 7. In Fig. 7, it is found that 5% and 10% cascade weight reductions achieved by changing vane configurations, resulted in reductions in total reverse thrust of 2.5% and 2.2% respectively.

Although reverse thrust is reduced by 2.5% and 2.2% for both of the reduced weight designs, the flow in the fan duct and around the cascade is subsonic flow. Fig. 8 shows the velocity vectors through a thrust reverser for the three cascade designs. It indicates similarity in the flow features around the cascade and in the fan duct. The directions of velocity while the flow passes through the cascade are nearly the same. However, in Fig. 8(a), it can be found that the supersonic flow is reached on the diverter fairing within the fan duct. There is no supersonic flow in the fan duct for both of the reduced weight cases (see Fig. 8 (b) and (c)). It means that the flow fields in the fan duct there are no shock waves on the diverter fairing for both weight reduction cases.

Also Fig. 9(a) shows the velocity contours colored by Mach number in the fan duct for cascade Design 1, with the thrust reverser engaged. Mach numbers above 1 are in red colored area and this plot shows that supersonic flow is reached on the diverter fairing during reverse thrust. The velocity contours for Design 2 and Design 3 are shown in Fig. 9(b) and (c). The same range of Mach number has been used for the three plots shown in Fig 9. The maximum Mach number in the fan duct is less than 1, in both of the reduced weight cases (i.e. Design 2 and 3) the flow in the fan duct is subsonic. Subsonic flow through the fan duct means that there is a reduced risk of the nacelle structure being subjected to the shock waves associated with the supersonic conditions predicted for Design 1.

Despite a reduction in total reverse thrust for the weight reduced designs, the supersonic flow regime, which existed in the original design, was eliminated after changing vane configurations made with the 5% and 10% weight reductions. Numerical simulations indicate that the total reverse thrust is not significantly affected with the modified cascade.

References

[1] Anon, Rolls Royce Aerospace Group, *The jet Engine*, Fifth edition, Renault Printing Co. Ltd., Birmingham, England, pp. 159-169, 1996.

[2] Polyméris J. Aviation operational measures for fuel and emissions reduction workshop. *Proceeding of Flight Operations Panel,* Madrid, Spain, pp 21-22, 2002.

[3] Scott C. Asbury & Jeffrey A. Yetter. Static Performance of a Wing-Mounted Thrust Reverser Concept. *AIAA 98-3256*, 1998.

[4] Luis Gustavo Trapp and Guilherem L. Oliveriram. Aircraft Thrust Reverser Cascade Configuration Evaluation Through CFD. *AIAA 2002-0723*, 2002.

[5] Butterfield J *et al.* Optimisation of a thrust reverser cascade: an assessment of dynamic response with a view to reducing weight. *3rd AIAA Annual Aviation Technology, Integration and Operation (ATIO) Technical Forum*, Denver, Colorado, USA, AIAA-2003-13526, 2003.

[6] Yao H, Benard E, Cooper R K, Raghunathan S, Tweedie J and Riordan D. Aerodynamics of natural blockage thrust reverser. *9th Aerodynamics Symposium*, Montreal, Canada, 239c, 2003.

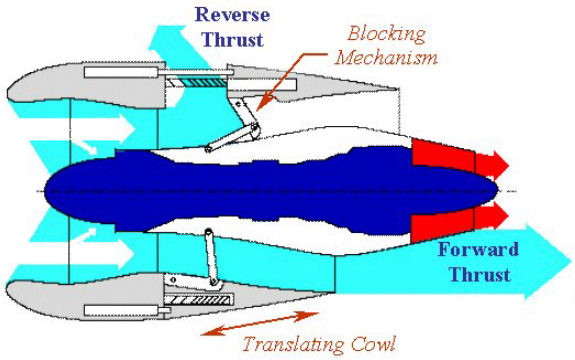

Fig. 1 A section through a typical cold stream thrust reverser

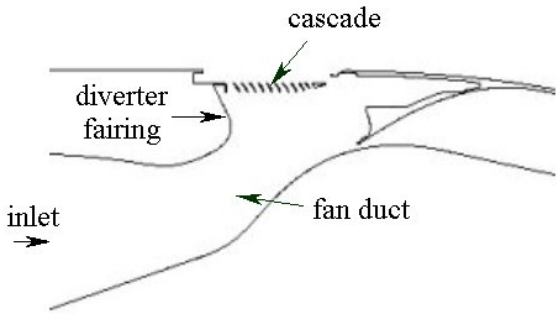

Fig. 2 Geometry of the thrust reverser computational fluid dynamics model

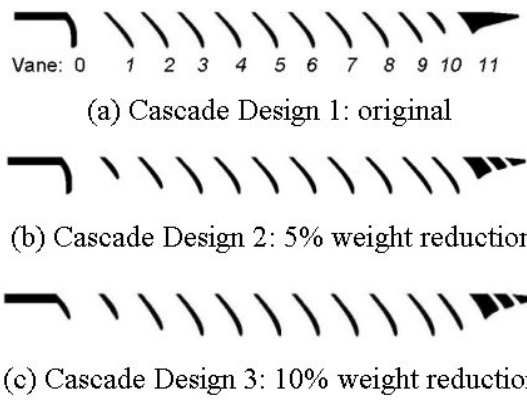

Fig. 3 Thrust reverser cascade for three design options

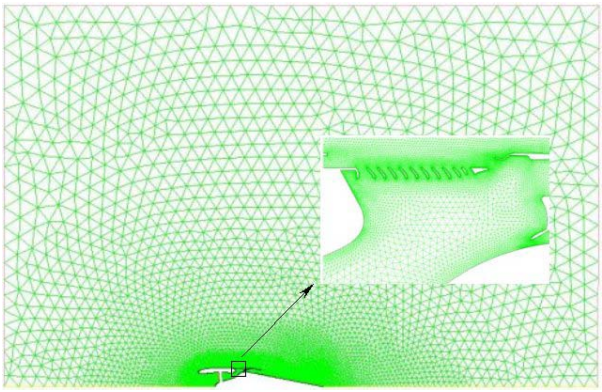

Fig. 4 Two-dimensional grid used to simulate flows through the thrust reverser

(a) Design 1, Original

(b) Design 2: 5% weight reduction

(c) Design 3, 10% weight reduction

Fig. 5 Static pressure distributions through the thrust reverser for three cascade designs

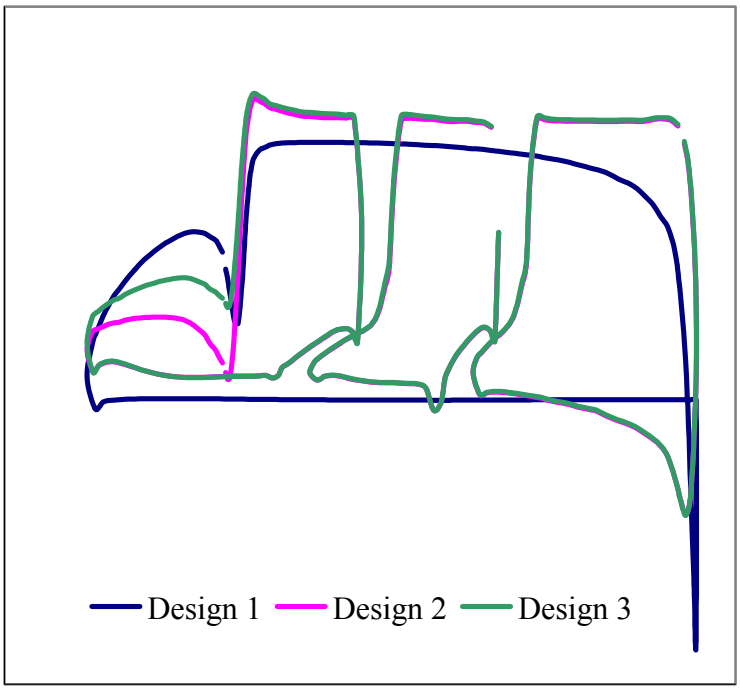

Fig. 6 Pressure distributions around Vane 11 for three cascade configurations

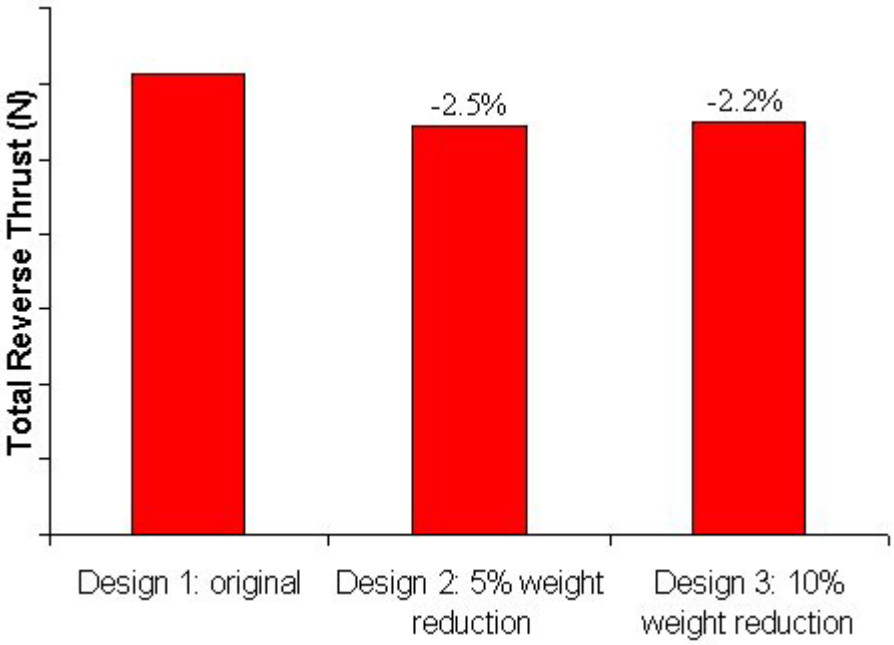

Fig. 7 Comparison of maximum total reverse thrust for three cascade configurations

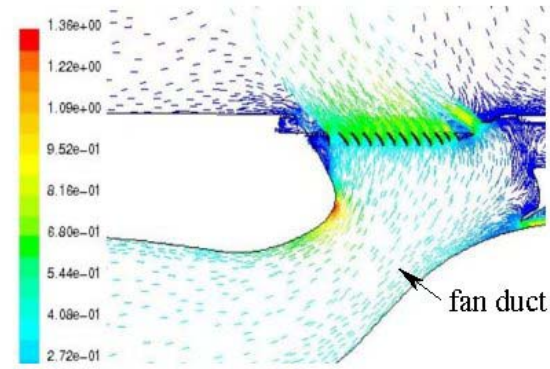

(a) Design 1, original

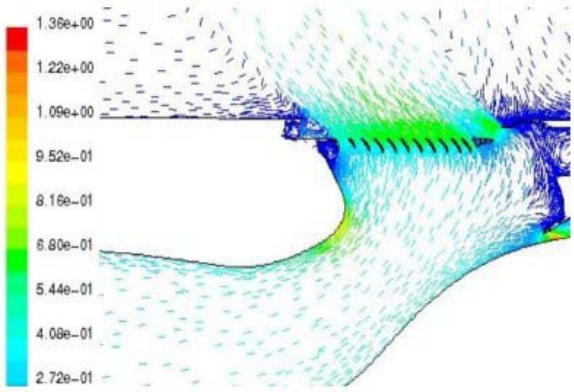

(b) Design 2, 5% weight reduction

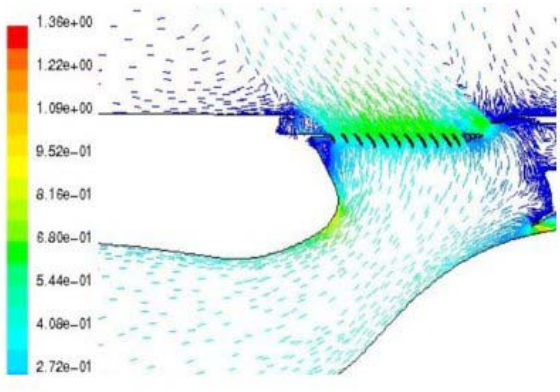

(c) Design 3, 10% weight reduction

Fig. 8 Velocity vectors colored by Mach number through the thrust reverser for three design options

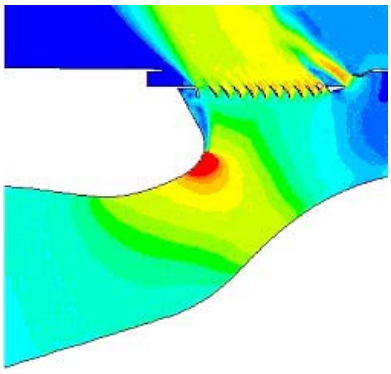

(a) Design 1, Original

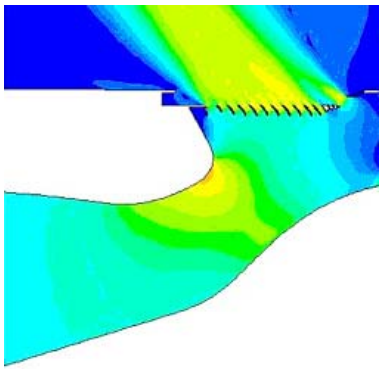

(b) Design 2, 5% weight reduction

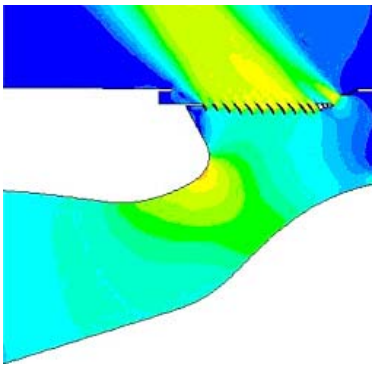

(c) Design 3, 10% weight reduction

Fig. 9 velocity contours colored by Mach number through the thrust reverser for three cascade designs